Opto-Electronic Properties of Poly (Fluorene) Co-Polymer Red Light-Emitting Devices on Flexible Plastic Substrate

Yongtaek Hong, *Member, IEEE*, and Jerzy Kanicki, *Senior Member, IEEE*

***Abstract*—In this paper, we report on the multilayer poly (fluorene) co-polymer red light-emitting devices (PLEDs) fabricated on flexible plastic substrates. An organic hole transport layer (HTL) is inserted between PEDOT:PSS hole injection (HIL) and light-emissive layers (LEL). Since the highest occupied molecular orbital (HOMO) of the HTL is located between those of HIL and LEL, the insertion of HTL reduces the effective HOMO level offset between HIL and LEL, reducing the device operation voltage and producing comparable or better device efficiencies in comparison with the conventional PEDOT:PSS-only devices. Maximum emission efficiency, ∼0.8 cd/A, power efficiency, ∼0.7 lm/W, and external quantum efficiency, ∼1.5%, have been obtained for multilayer red PLEDs.**

***Index Terms*—Multilayer structure, organic polymer red light-emitting devices (PLEDs), plastic substrate.**

I. Introduction

TODAY, ORGANIC light-emitting device (OLED) technology is believed to be one of the most promising candidates for flexible passive- and active-matrix flat panel displays (FPDs) [1] because OLEDs can be easily fabricate over large-area plastic substrates at low temperature and low cost. Gustafsson *et al.* [2] fabricated fully flexible polymer LED on poly (ethylene terephthalate) (PET) substrates in 1992. They used polyaniline anode for their devices to overcome the brittle properties of indium–tin–oxide (ITO). In 1997, Gu *et al.* [3] successfully demonstrated vacuum-deposited OLEDs on ITO-coated polyester substrates. They reported that the flexible OLEDs did not deteriorate after repeated bending. Recently, a fluorine-containing polyimide substrate has been used for the vacuum-deposited OLEDs [4]. A standard sputtering method was used to deposit an ITO layer, whose optical, electrical, and surface characteristics were optimized by setting the substrate temperature very high (up to 200 °C) during the ITO sputtering. In all three cases, the opto-electronic performance of the devices was comparable to that of the OLEDs fabricated on ITO-coated glass substrates. However, if the ITO layer on plastic substrate is differently deposited and/or its surface is differently treated during etching or cleaning processes, the ITO electrical property and surface roughness can be degraded, resulting in poorer device opto-electronic performance in comparison with the devices on the ITO-coated glass substrate [5], [6].

For the past several years, we have also investigated the organic polymer LEDs (PLEDs) on flexible plastic substrates [7]–[9]. The high-quality ITO-coated flexible plastic substrates used in our research are based on poly [bis(cyclopentadiene) condensate]s—"transphan" [10], which can be a good substrate candidate for flexible FPDs, along with the previously reported barrier-coated PET plastic substrate [11]. They both have a low ITO surface roughness (< 20 Å root mean square) and a low sheet resistance ($< 50\ \Omega/\square$), and very low water vapor ($< 10^{-6}$ g/cm^2-day-atm) and oxygen ($< 10^{-7}$ cc/cm^2-day-atm) transmission rates, which are very desirable properties for the flexible OLED/PLED displays [12], [13].

In this paper, we report on the opto-electronic properties of red poly (fluorene) co-polymer based multilayer PLEDs fabricated on the flexible plastic substrate [10]. A thin organic hole transport layer (HTL) was inserted between an aqueous hole injection layer (HIL) and a light-emissive layer (LEL) to effectively reduce the highest occupied molecular orbital (HOMO) level offsets between HIL and LEL and to confine electrons at the HTL and LEL interface. The inserted HTL results in a reduced device operational voltage with comparable or higher device efficiency. This type of multilayer approach (HIL/HTL) has been used for vacuum deposited OLEDs to improve hole injection properties and thus, to reduce operation voltage and to enhance opto-electronic performance of the device [14]–[16]. In addition to the enhanced opto-electronic performance, the inserted organic HTL is expected to protect LEL from water left or reabsorbed in an aqueous HIL and further reduce the indium contamination from ITO into LEL. Both reductions can enhance the PLED operation stability and lifetime.

II. Experimental Details

A. PLED Fabrication

Fig. 1 shows the structure of the multilayer PLEDs fabricated on the flexible plastic substrate [10]. ITO and calcium–aluminum (Ca–Al) bi-layer were used as anode and cathode metals, respectively. The ITO prepatterned plastic substrate was cleaned in the ultrasonic bath of isopropanol for 20 min. ITO is highly conductive n-type material and transparent to the visible light due to its high carrier density ($\sim 10^{21}$ cm^{-3}) and

Manuscript received March 22, 2004. This work was supported by the National Institutes of Health, Bethesda, MD. The review of this paper was arranged by Editor M. Anwar.

Y. Hong was with the Solid-State Electronics Laboratory, Department of Electrical Engineering and Computer Science, University of Michigan, Ann Arbor, MI 48105 USA. He is currently with the Display Science and Technology Center, Eastman Kodak, Rochester, NY 14650 USA (e-mail: yongtaek.hong@kodak.com).

J. Kanicki is with the Solid-State Electronics Laboratory, Department of Electrical Engineering and Computer Science, University of Michigan, Ann Arbor, MI 48105 USA (e-mail: kanicki@eecs.umich.edu).

Digital Object Identifier 10.1109/TED.2004.835161

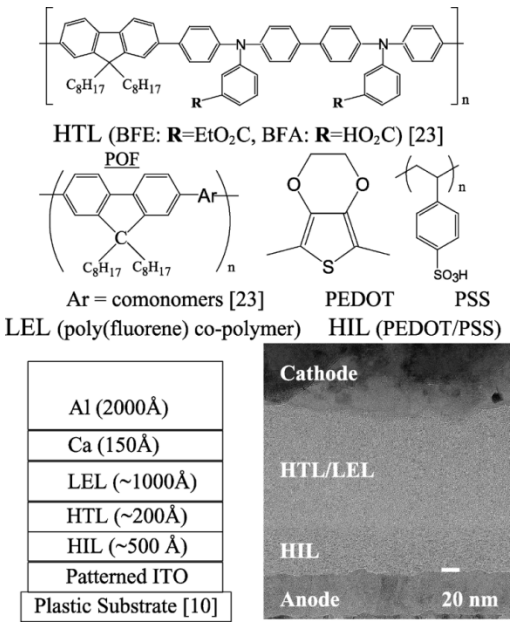

Fig. 1. PLED multilayer structure used in this study is shown. The chemical structures of all organic materials and an example of the high-resolution TEM cross-section images for multilayer PLED are also included.

wide bandgap (3.5–4.3 eV) [17]. For OLEDs, ITO is typically used as anode electrode due to its high work function (∼4.8 eV) and transparency [18]. The interfacial energy barrier plays an important role in the device performance such as operation voltage. Since the work function of ITO and Fermi-level energy are sensitive to the surface conditions, the ITO surface treated by various methods, such as plasma or UV-ozone treatment, has been extensively studied in recent years [19]–[22]. In this study, before organic polymer layer was deposited, the ITO surface was exposed to UV-ozone treatment for 20 min. This type of ITO treatment will enrich the negatively charged oxygen on the ITO surface, which increases the ITO work function [22]. The treatment also enhances the ITO surface wetting property by removing organic carbon contaminants and changing ITO surface energy and polarity [21]. We observed that after UV-ozone treatment, the advancing contact angles of our ITO patterned plastic substrate reduced for water ($\sim$ 40° reduction) and methylene iodine ($\sim$ 15° reduction) [10]. The reduction of the contact angle implies the increase of the polarity and surface energy, which is believed to improve the interface formation between ITO and polymer layers [21].

On the UV-ozone treated ITO, we spun-coated poly (3, 4-ethylene dioxythio phene) doped with poly (styrenesulfonate) (PEDOT:PSS, Baytron P as purchased from Bayer, Germany) and cured for 20 min at 90 °C in the vacuum oven (aqueous HIL, $\sim$ 500 Å). Then, poly (9,9-dioctylfluorene-co-N,N′-di (phenyl)-N,N′-di (3-carbo ethoxyphenyl) benzidine (BFE) [23] in xylene solution were spun-coated and cured for one hour at 90 °C in the vacuum oven (organic HTL, $\sim$ 200 Å). After that, we spun-coated red light-emitting poly (fluorene) copolymer [23] in xylene solution and cured for 1 h at 90 °C in the vacuum oven (LEL, ∼800 or $\sim$ 1000 Å). All the spin-coating processes were performed at room temperature in the air. Finally, a Ca–Al (150 Å/2000 Å) bi-layer cathode was thermally evaporated through a shadow mask without

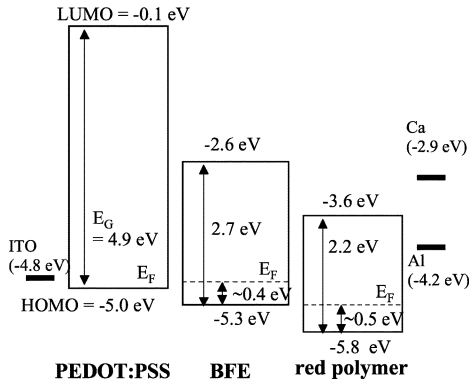

Fig. 2. Schematic energy band diagram for multilayer PLED before the electrical contact is shown, where all the energy values are relative to the vacuum level. HOMO levels are obtained from CV data and LUMO levels are calculated from the optical bandgap extracted from Tauc plots.

breaking vacuum under $\sim 10^{-6}$ torr. The fabricated PLED size was 0.1×0.1 in^2. To compare the device performances, aqueous HIL ($\sim$ 500 Å) PEDOT:PSS-only and organic HTL poly (9,9-dioctylfluorene-co-N,N′-di(phenyl)-N,N′-di(3-carboxyphenyl)benzidine (BFA) (400–500 Å)-only PLEDs were also fabricated and measured. The chemical structures of materials used in this study and an example of the high-resolution ($\times$ 250 000) transmission electron microscopy (TEM) images for inorganic HIL/organic HTL multilayer PLED are also included in Fig. 1.

B. PLED Measurement

The opto-electronic properties of PLEDs were measured in the air at room temperature with an integrating sphere-based measurement system [24], in which a programmable voltage source (Keithley 230) and an electrometer (Keithley 617) were used for electrical signal forcing and measurement. IL1700 Research Radiometer from International Light and CCD3000 from JY Horiba were used for luminous and quantum efficiency measurement, respectively. The fabricated devices were mounted on the input port of the integrating sphere and then all the electrical and optical measurements were simultaneously performed.

III. Experimental Results and Discussion

A. PLED Energy Band Diagram

Fig. 2 shows the energy band diagram of the multilayer red light-emitting PLED before the electrical contact. The work function of ITO [18], Ca [25], and Al [25] are also included. The energy band diagram of BFE and red poly (fluorene) co-polymer is constructed from a combination of cyclic voltammetry (CV) and optical data for the materials used in the PLEDs [26]. We are assuming that organic polymers used in this study behave like organic semiconductors. The positions of the average highest occupied molecular orbital (HOMO) levels (BFE: ~ -5.3 eV, red: ~ -5.8 eV) are in a good agreement with the HOMO levels of the poly (fluorene) based co-polymers reported elsewhere [23], [27]. The Fermi levels of BFE and red poly (fluorene) co-polymer were assumed to have similar activation energies (∼0.4 and ∼0.5 eV, respectively) to the previously reported poly (fluorene) co-polymers [9]. Since the CV spectrum of PEDOT:PSS was not available, -5.0 eV [18]

is used as its HOMO level. The Fermi level of PEDOT/PSS is assumed to be located very close to or at its HOMO level. The LUMO level of PEDOT:PSS, BFE, and red polymer were estimated from the optical bandgaps, which are obtained from the Tauc plots [26] that represent the relationship between absorption coefficient and photon energy for three-dimensional amorphous semiconductor structure [28], [29]. The extracted LUMO levels of PEDOT:PSS, BFE, and red polymer with respect to the vacuum energy levels are ~ -0.1, ~ -2.6, and ~ -3.6 eV, respectively.

B. Engineering of HOMO Level Offset of Red PLED

For a conventional PEDOT:PSS-only bi-layer red PLED, the work function of Ca (-2.9 eV) and the PEDOT:PSS HOMO level (-5.0 eV) are smaller than the LUMO (-3.6 eV) and HOMO (-5.8 eV) levels of red polymer, respectively. Therefore, for this device, it is speculated that the electron extraction (hole injection) process through the HOMO level offset between PEDOT:PSS and red polymer can limit the PLED opto-electronic characteristics in comparison with the electron injection through the offset between red polymer LUMO level and Ca work function. Although the transport properties of the charged carriers in PLEDs can also affect the device performances, it has been reported that if the carriers injection rates are different, the device performances are limited by the carrier with the larger injection (or extraction) barrier (in our case, electron extraction (hole injection) HOMO level offset at PEDOT:PSS-red polymer interface) and the carriers transport characteristics (carriers mobility) are less important [30].

In addition, it is noted that chemical interactions and/or interfacial layer formation can occur at polymer/metal interfaces, affecting the device opto-electronic performances [31], [32]. Therefore, it is important to take into account the interfacial electronic characteristics to engineer and optimize the device structure for better electrical and optical device performance. However, it is known that the size of the carrier injection barrier still scales with the energy differences between metal work functions and polymer HOMO/LUMO levels although the energy band bending and/or the interfacial states exist at the interfaces [33].

In this paper, by inserting a BFE layer between PEDOT:PSS and red polymer layers, the HOMO level offset between PEDOT:PSS and red polymer is effectively reduced from $\sim$0.8 eV to two steps of $\sim$0.3 and $\sim$0.5 eV. This reduction of the HOMO level offsets can cause the electric field redistribution preferable for hole injection/transport in the device, which can result in larger current at a given voltage under forward bias; thus, a reduction of the device operation voltage. It should be noted that the inserted BFE layer provides a large ($\sim$1 eV) LUMO level offset with respect to red polymer, which can effectively confine electrons at the interface in between, hindering electrons from leaving red polymer layer without radiative recombination with holes. Therefore, the multilayer red PLED is expected to have a lower operation voltage and comparable or better device efficiencies in comparison with the conventional PEDOT:PSS-only device. The opto-electronic characteristics of the multilayer and PEDOT:PSS-only PLEDs under forward bias will be further discussed later.

In addition to the staircase-like HOMO level offset engineering, an intermixing occurs between BFE and red polymer in multilayer PLEDs during the device fabrication. The intermixed layer formation can have a positive effect on the device opto-electronic performances, which is similar to the graded-junction between HTL and LEL in the case of vacuum-evaporated molecular organic light-emitting devices [34], [35]. The graded-junction reduces electroluminescence quenching cation and redistributing electrical field in the device, resulting in an enhancement of the device operational stability [34] and efficiencies [35]. For PLEDs, the graded HOMO levels in HIL have been used to improve hole injection in LEL, especially poly (fluorene) co-polymer based LEL, which produces a high HOMO level offset between HIL and LEL [36]. In addition, a thin electron confinement layer was inserted between graded HIL and LEL to enhance the opto-electronic performance of the device [36], [37]. It should be noted that, in our multiplayer PLEDs, a thin HTL plays both roles of reducing HOMO level offset between HIL and LEL, and confining electrons at the HTL and LEL interface.

C. Current Density-Voltage Characteristics

Fig. 3(a) shows current density versus voltage (*J–V*) characteristics for PEDOT:PSS-only and PEDOT:PSS/BFE multilayer PLEDs with different LEL thicknesses. The PLED with a thick (~ 1000 Å) LEL shows a lower current density in comparison with the PLED with a thin (~ 800 Å) LEL for a given applied voltage. At 7 V, for PEDOT:PSS-only PLEDs, the current densities of $\sim$80 and ~ 170 mA/cm^2 have been obtained for thick and thin LEL thickness, respectively. For PEDOT:PSS/BFE multilayer PLEDs, $\sim$120 and $\sim$ 220 mA/cm^2 have been obtained for thick and thin LEL thickness, respectively, at the same applied voltage. In our PLEDs, the increase of the LEL thickness by $\sim$ 200 Å, thus the increase of the total active organic polymer layer between anode and cathode by the same amount, causes a current density reduction for the same applied voltage by approximately factor of two for both PEDOT:PSS-only and PEDOT:PSS/BFE multilayer PLEDs. However, when we compare PEDOT:PSS-only and PEDOT:PSS/BFE multilayer PLEDs for the same LEL thickness, a higher current density at the same applied voltage has been observed for PEDOT:PSS/BFE multilayer PLEDs although the thickness of the total active organic polymer layer between anode and cathode increases by the thickness ($\sim$ 200 Å) of the inserted BFE layer. It is speculated that the inserted HTL of BFE, which has its HOMO level between the HOMO levels of PEDOT:PSS and red polymer, effectively reduces the HOMO level offsets between PEDOT:PSS and red polymer and causes a modification of the internal electric field, facilitating injection/transport of carriers through the device. It is noted that the off-current density of our PLEDs at applied voltages lower than $\sim$2 V is further reduced by increasing the LEL thickness and is not severely modified by the insertion of BFE HTL layer as shown in log-linear plot of *J–V* characteristics, Fig. 3(a).

In our PLEDs, the *J–V* characteristics cannot be simply described by a pure injection or a pure transport model, such as

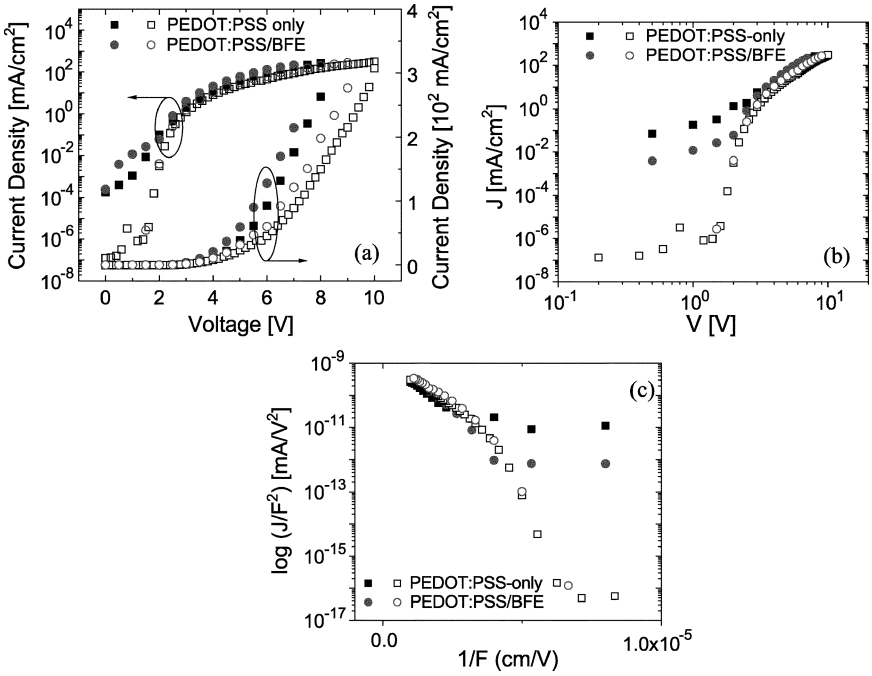

Fig. 3. Current density versus voltage characteristics of PLEDs. (a) Linear and semilog plot, (b) log–log plot for SCLC and TCL model fitting, and (c) semilog plot for FN tunneling model fitting are shown. Squares and circles are for PEDOT:PSS-only and PEDOT/BFE multilayer PLEDs. Solid and open symbols represent the measured data for PLEDs with thin (~ 800 Å) and thick (~ 1000 Å) LEL, respectively.

space charge limited current (SCLC) [38], trapped charge limited current (TLC) [39], or simple Fowler–Nordheim (FN) tunneling [40]. These models are characterized by the following relationships between the current density and the applied voltage:

$$J \propto V^2 \quad \text{(SCLC)} \tag{1}$$

$$J \propto V^{m+1}, \quad \text{m} > 1 \quad \text{(TLC)} \tag{2}$$

$$\ln\left(\frac{J}{F^2}\right) \propto -\frac{1}{F}, \quad F = \frac{V}{d} \quad \text{(FN tunneling)} \tag{3}$$

where, d is the thickness of PLEDs. The *J–V* characteristics of our PLEDs were not fitted to one of the above relationships over several orders of magnitude for PLED current density as shown in Fig. 3(b) and (c). Therefore, none of these mechanisms are solely responsible for the *J–V* characteristics of our PLEDs. Most likely, a combination of the different conduction processes can explain the electrical behavior of the PLEDs. To further investigate the effect of the modified HOMO level offsets on the opto-electronic properties of the PLEDs, the light-emission properties are carefully studied in the next section.

D. Opto-Electronic Characteristics

Luminance versus Voltage and Current Density Characteristics: Fig. 4(a) shows the luminance versus voltage (*L–V*) characteristics for the fabricated PLEDs. The light-emission was initially detected at 2–2.5 V for both PEDOT:PSS-only and PEDOT:PSS/BFE multilayer PLEDs. However, as the applied voltage increases, enhanced light-emission was observed for PEDOT:PSS/BFE multilayer PLEDs at the same applied voltage. At 7 V, for PEDOT:PSS-only PLEDs, the luminance of $\sim$580 and $\sim$ 800 cd/m^2 have been obtained for thick and thin LEL thickness, respectively. For PEDOT:PSS/BFE multilayer PLEDs, $\sim$800 and $\sim$ 1200 cd/m^2 have been obtained for thick and thin LEL thickness, respectively, at the same applied voltage. It is speculated that, the hole transport over the HOMO level offset between PEDOT:PSS and red polymer is limiting factor for the PEDOT:PSS-only PLEDs because the inserted BFE HTL increases not only the current density as described in the previous section but also the light-emission at a given applied voltage. The reduced effective HOMO level offset between PEDOT:PSS and red polymer layers modifies the internal electric field distribution that enhances hole injection/transport over the HOMO level offsets at the polymer interfaces. This will contribute to increased current density and luminance at a given applied voltage. We also plotted luminance versus current density (*L–J*) characteristics in Fig. 4(b). For *L–J* characteristics, the corresponding current density and luminance were taken from Fig. 3(a) and Fig. 4(b) at a given applied voltage, respectively. A comparable or better light-emission was obtained at the same current density for the PEDOT:PSS/BFE multilayer PLEDs in comparison with the PEDOT:PSS-only PLEDs. Although an increase of current density at a given applied voltage was observed, only slight increase of light-emission was obtained at a given current density for PEDOT:PSS/BFE multilayer PLEDs. However, we believe that the optimization of each layer thickness can further enhance *L* values for a given *J*. The *L–J* curves shown in Fig. 4(b) can be described by the following equation. No saturation of *L–J* characteristics was observed for the measured data

$$L \propto J^{\alpha} (\alpha = 1.02 \pm 0.02). \tag{4}$$

It is also noted that the enhanced light-emission was obtained for thicker LEL devices; thus, we can also engineer the device structure for better opto-electronic performances by optimizing LEL thickness. However, as the thickness of LEL increases in the PLED structure, the voltage values required for given current

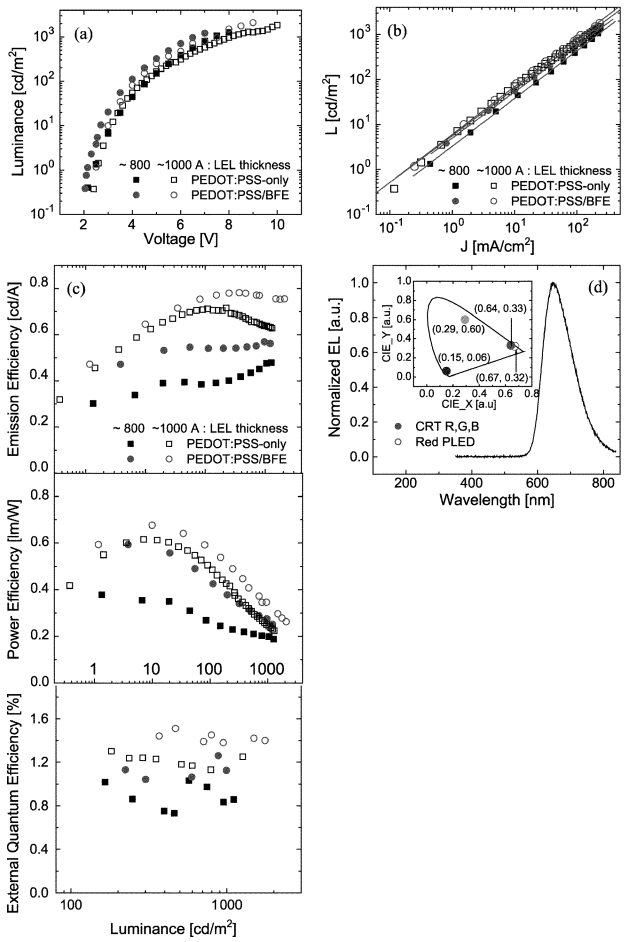

Fig. 4. Opto-electronic characteristics of PEDOT:PSS-only and PEDOT:PSS/BFE multilayer PLEDs. (a) Luminance versus voltage, (b) luminance versus current density, (c) emission efficiency versus luminance, (d) power efficiency versus luminance, and (e) external quantum efficiency versus luminance are shown. (f) CIE color coordinates of PEDOT:PSS/BFE multilayer PLEDs with thick (~ 1000 Å) LEL was calculated from measured EL spectrum.

density levels increase as shown in Fig. 3(a). This is more clearly shown in the *L–V* characteristics, Fig. 4(a). Therefore, instead of increasing the LEL thickness, the insertion of thin HIL can be a more effective method in improving the device efficiencies.

EE Versus Luminance Characteristics: Fig. 4(c) shows the emission efficiency (EE) versus luminance characteristics of the fabricated PLEDs. EE is defined as the ratio of the PLED luminance (*L*) to the input current density (*J*) as shown in the following equation:

$$\mathrm{EE} = \frac{L}{J} \tag{5}$$

where *L* and *J* were obtained from Fig. 4(a).

Enhanced EE was obtained for PEDOT:PSS/BFE multilayer PLEDs in comparison with PEDOT:PSS-only PLEDs for both thin and thick LEL devices, as shown in Fig. 4(c). For thick LEL PLEDs, the stable emission efficiency of ~0.8 cd/A was obtained over the luminance ranging of from ~100 to $\sim$ 1000 cd/m^2 for PEDOT:PSS/BFE multilayer PLEDs while the PEDOT:PSS-only PLEDs showed the maximum EE of ~0.7 cd/A at $\sim$ 100 cd/m^2 and a decreasing EE for larger luminance. Therefore, the PEDOT:PSS/BFE multilayer PLEDs can be operated with a higher EE over large range of *L*.

PE Versus Luminance Characteristics: Fig. 4(c) shows the power efficiency (PE) versus luminance characteristics of the fabricated PLEDs. The PE is defined as the ratio of the PLED total luminous flux (Φ) to the input electrical power, which was obtained by dividing the measured total luminous flux by the product of the corresponding input current (*I*) and voltage (*V*) as shown in the following equation:

$$\mathrm{PE} = \frac{\Phi}{IV} = \frac{\pi L}{JAV} = \frac{\pi EE}{AV} \tag{6}$$

where *A* is the PLED area. The obtained PE shows a typical parabolic curve as the luminance increases because higher voltage (thus higher input electrical power) is required as the luminance increases. Enhanced PE was obtained for PEDOT:PSS/BFE multilayer PLEDs in comparison with PEDOT:PSS-only PLEDs for both thin and thick LEL devices, as shown in Fig. 4(c). The maximum PE of ~0.7 lm/W was obtained at $\sim$ 10 cd/m^2 for PEDOT:PSS/BFE multilayer PLEDs with the thick LEL.

EQE Versus Luminance Characteristics: Fig. 4(c) shows the external quantum efficiency (EQE) versus luminance characteristics of the fabricated PLEDs. The EQE is defined as the ratio of the number of the emitted photons to the number of the input electrons. The number of the emitted photons was calculated by dividing the PLED optical power spectral distribution $(P(\lambda))$ by the photon energy $(h\nu = \mathrm{hc}/\lambda)$ at each wavelength and then, by integrating it over the measured wavelength as shown in the following equation:

$$\mathrm{EQE} = \frac{\int \left(\frac{P(\lambda)}{\left(\frac{hc}{\lambda}\right)} \right) d\lambda}{\left(\frac{I}{q}\right)} \tag{7}$$

where *h, c,* and *q* are Plank constant, light velocity, wavelength, and charge of an electron, respectively.

The PLED optical power spectral distribution was measured by using the CCD-based measurement setup at several applied voltages. The detailed procedure has been published elsewhere [24]. Consistently, enhanced EQE was obtained for PEDOT:PSS/BFE multilayer PLEDs in comparison with PEDOT:PSS-only PLEDs for both thin and thick LEL devices, as shown in Fig. 4(c). The maximum EQE of ~1.5% was obtained at $\sim$ 400 cd/m^2 for PEDOT:PSS/BFE multilayer PLEDs with the thick LEL and stable EQE was observed for *L* ranging from ~200 to $\sim$ 1100 cd/m^2.

CIE Color Coordinates: The insert of Fig. 4(f) shows the Commission Internationale de l'Eclairage (CIE) chromaticity coordinates [41] for PEDOT:PSS/BFE multilayer PLEDs with the thick LEL, which is calculated from EL spectrum by using a software previously developed in our group. The software calculates three fundamental tristimulus values (*X, Y,* and *Z*) by integrating products of the measured EL and each of the three eye response curves [41] and then, averages out *X, Y*, and *Z* values to produce *x, y,* and z ($x = X/(X+Y+Z)$, $y = Y/(X+Y+Z)$, $z = Z/(X+Y+Z)$). Since the sum of *x, y*, and *z* is unity, *z* can be always calculated from *x* and y values, which are commonly

TABLE I
OPTO-ELECTRONIC CHARACTERISTICS OF VARIOUS PLEDS (LEL: $900 \sim 1000$ Å) FABRICATED ON PLASTIC SUBSTRATE ARE SUMMARIZED IN COMPARISON WITH RED LIGHT-EMITTING POLY (FLUORENE) BASED PLED ON GLASS SUBSTRATES, WHICH ARE REPORTED FROM CDT [42], [43] AND DOW CHEMICAL COMPANY [44] (*LIFETIME IS DEFINED AS THE TIME ELAPSED WHEN THE DEVICE INITIAL LUMINANCE 100 cd/m^2 IS REDUCED TO ITS HALF VALUE 50 cd/m^2)

		BFA-only	PEDOT-only	PEDOT /BFE	CDT	DOW
Substrate		plastic	plastic	plastic	glass	glass
Process environment		air	air	air	nitrogen	nitrogen
Packaging		no	no	no	yes	yes
100 cd/m^2	cd/A	0.7	0.7	0.8	1.7	N/A
	lm/W	0.3	0.5	0.6	1.2	N/A
	V	6.8	4.6	4	2.4	N/A
	mA/cm^2	18	15.3	13	6	N/A
200 cd/m^2	cd/A	0.7	0.7	0.8	N/A	1.3
	lm/W	0.3	0.4	0.5	N/A	1.1
	V	7.7	5.3	4.5	N/A	3.6
	mA/cm^2	34	29	26	N/A	16
1000 cd/m^2	cd/A	0.6	0.6	0.8	1.1	0.9
	lm/W	0.15	0.2	0.4	0.7	0.5
	V	10.7	8.2	7.5	5.4	6.2
	mA/cm^2	165	165	130	99	110
Peak EE	cd/A	0.7	0.7	0.8	1.7	1.3
Peak PE	lm/W	0.3	0.5	0.6	1.2	1.1
Peak EQE	%	1.3	1.3	1.5	3	N/A
CIE	(x, y)	(0.67, 0.32)	(0.67,0.32)	(0.67, 0.32)	(0.67, 0.33)	(0.68, 0.31)
Lifetime*	L_0, 100 cd/m^2	N/A	N/A	N/A	> 40,000 hrs	~ 5,500 hrs

used to plot the CIE chromaticity coordinates for the measured light source. The obtained CIE chromaticity coordinates for the multilayer PLEDs with the thick LEL are (0.67, 0.32). In comparison with National Television System Committee (NTSC) red (R), green (G), and blue (B) color coordinates, our device shows a very saturated red color that can be used for full color PLED-based flat panel displays.

Other Devices: We also fabricated HTL-only ($400 \sim 500$ Å) devices with the thick (~ 1000 Å) LEL. BFE in xylenes and poly (9,9-dioctylfluorene-co-N,N′-di(phenyl)-N,N′di(3-carboxy phenyl)benzidine) (BFA) [23] in dimethylformamide (DMF) were used as HTL materials. BFA has similar energy band structure (~ -5.3-eV HOMO levels and $\sim$2.7-eV optical bandgap) to BFE but is not soluble in xylene. The BFA HTL-only devices showed similar EE and EQE, but lower PE, in comparison with PEDOT:PSS HIL-only devices. The lower PE of BFA HTL-only PLEDs comes from the higher operation voltage of the device in comparison with PEDOT:PSS-only PLEDs. The BFA HOMO level gives a larger offset with respect to the ITO work function than PEDOT:PSS HOMO level by $\sim$0.3 eV, while the BFA HOMO level forms a smaller offset with respect to the red polymer HOMO level than PEDOT:PSS by the same amount ($\sim$0.3 eV). Based on the obtained result for BFA HTL- and PEDOT:PSS-only PLEDs, the energy offset at the ITO/polymer interface may be more important than at the polymer/polymer interface to reduce the device operation voltage. The BFE HTL-only device produced very poor device performances. It is speculated that intermixing during the LEL spin-coating can degrade the contact property between ITO and BFE, resulting in device performance degradation. We also inserted the BFA HTL layer between PEDOT:PSS and LEL, but the PEDOT/PSS layers seemed to be attacked by the DMF solution and spin-coated film quality was not good enough for device performance evaluation. Table I summarizes the obtained results for various PLEDs fabricated on plastic substrates.

Finally, our multilayer PLED opto-electronic performances are also compared with red light-emitting poly (fluorene) based PLED fabricated on glass substrates, which are reported from Cambridge Display Technology (CDT) [42], [43] and Dow Chemical Company [44]. It is noted that since our PLEDs are fabricated in the air, all the interfaces are exposed to air during the device fabrication. It is well known that the device performance characteristics can be degraded when the light-emitting polymer is exposed to air [45]. In addition, ITO electrical and surface characteristics vary for different types of ITO surface treatment, resulting in device performance variations [22]. Therefore, it is very difficult to directly compare the device performances with each other due to the process/measurement environmental sensitivity of PLEDs performances. Although our PLEDs on plastic substrates generally show lower device efficiencies in comparison with the reported devices on glass substrates by a factor of one or two, to the best of our knowledge, the opto-electronic performance of the red light-emitting PLED on the flexible plastic substrate was investigated in this paper for the first time.

IV. CONCLUSION

We reported on the multilayer poly (fluorene) co-polymer red light-emitting PLEDs on flexible plastic substrates. By combining aqueous PEDOT:PSS HIL and organic BFE HTL between ITO anode and the LEL in the device structure, we successfully reduced the effective HOMO level offsets between

HIL and LEL. In comparison with the PEDOT/PSS-only device, increased current density and improved device efficiency have been obtained, which show that our red PLED is a hole injection/transport limited device. Enhanced device performances of maximum emission efficiency ~0.8 cd/A, power efficiency ~0.7 lm/W, and external quantum efficiency ~1.5% have been obtained for the PEDOT:PSS/BFE multilayer PLED with the thick ($\sim$ 1000 Å) LEL for the thermally evaporated Ca–Al bi-layer cathode.

ACKNOWLEDGMENT

The authors would like to thank A. Johnson at the University of Michigan for BFA and BFE HOMO level measurements.

REFERENCES

[1] J. J. Brown and G. Yu, "Flexible OLED displays," in *SID Tech. Dig.*, vol. 34, 2003, pp. 855–872.
[2] G. Gustafsson, Y. Cao, G. M. Treacy, F. Kavetter, N. Colaneri, and A. J. Heeger, "Flexible light-emitting diodes made from soluble conducting polymers," *Nature*, vol. 357, pp. 477–479, 1992.
[3] G. Gu, P. E. Burrows, S. Venkatesh, S. R. Forrest, and M. E. Thompson, "Vacuum-deposited, nonpolymeric flexible organic light-emitting devices," *Opt. Lett.*, vol. 22, no. 3, pp. 172–174, 1997.
[4] H. Lim, W. J. Cho, C. S. Ha, S. Ando, Y. K. Kim, C. H. Park, and K. Lee, "Flexible organic electroluminescent devices based on fluorine-containing colorless polyimide substrates," *Adv. Mater.*, vol. 14, no. 18, pp. 1275–1279, 2002.
[5] J. Zhao, S. Xie, S. Han, Z. Yang, L. Ye, and T. Yang, "A bilayer organic light-emitting diode using flexible ITO anode," *Phys. Stat. Sol. A*, vol. 184, no. 1, pp. 233–238, 2001.
[6] S. H. Kwon, S. Y. Paik, and J. S. Yoo, "Electroluminescent properties of MEH-PPV light-emitting diodes fabricated on the flexible substrate," *Synth. Met.*, vol. 130, pp. 55–60, 2002.
[7] Y. Hong, Z. Hong, and J. Kanicki, "Materials and devices structures for high performance poly OLEDs on flexible plastic substrates," *Proc. SPIE*, vol. 4105, pp. 356–361, 2000.
[8] Y. Hong, Z. He, S. Lee, and J. Kanicki, "Air-stable organic polymer red light-emitting devices on flexible plastic substrates," *Proc. SPIE*, vol. 4464, pp. 329–335, 2001.
[9] Y. He and J. Kanicki, "High efficiency organic polymer light-emitting devices on the flexible plastic substrates," *Appl. Phys. Lett.*, vol. 76, no. 6, pp. 661–663, 2000.
[10] Y. Hong, Z. He, L. S. Lennhoff, D. Banach, and J. Kanicki, "Flexible plastic substrates for organic light-emitting devices and other devices," *J. Electron. Mater.*, vol. 33, no. 4, pp. 312–9320, 2004.
[11] P. E. Burrows, G. L. Graff, M. E. Gross, P. M. Martin, M. K. Shi, M. Hall, E. Mast, C. Bonham, W. Bennett, and M. B. Sullivan, "Ultra barrier flexible substrates for flat panel displays," *Displays*, vol. 22, pp. 65–69, 2001.
[12] J. K. Mahon, J. J. Brown, T. X. Zhou, P. E. Burrows, and S. R. Forrest, "Requirements of flexible substrates for organic light emitting devices in flat panel display applications," in *Proc. Annu. Tech. Conf. Soc. Vacuum Coaters*, 1999, pp. 456–459.
[13] P. E. Burrows, G. L. Graff, M. E. Gross, P. M. Martin, M. Hall, E. Mast, C. Bonham, W. Bennett, L. Michalski, M. Weaver, J. J. Brown, D. Fogarty, and L. S. Sapochak, "Gas permeation and lifetime tests on polymer-based barrier coatings," *Proc. SPIE*, vol. 4105, pp. 75–83, 2000.
[14] S. A. Van Slyke, C. H. Chen, and C. W. Tang, "Organic electroluminescent devices with improved stability," *Appl. Phys. Lett.*, vol. 69, no. 15, pp. 2160–2162, 1996.
[15] X. Zhou, M. Pfeiffer, J. Blochwitz, A. Werner, A. Nollau, T. Fritz, and K. Leo, "Very-low-operating-voltage organic light-emitting diodes using a p-doped amorphous hole injection layer," *Appl. Phys. Lett.*, vol. 78, no. 4, pp. 410–412, 2001.
[16] F. Zhang, A. Petr, U. Kirbach, and L. Dunsch, "Improved hole injection and performance of multiplayer OLED devices via electrochemically prepared-polybithiophene layers," *J. Mater. Chem.*, vol. 13, pp. 265–267, 2003.
[17] J. H. Lan and J. Kanicki, "Patterning of transparent conducting oxide thin films by wet etching for a-Si:H TFT-LCDs," *J. Electron. Mater.*, vol. 25, no. 12, pp. 1806–1817, 1996.
[18] R. Friend, J. Burroughes, and T. Shimoda, "Polymer diodes," *Phys. World*, pp. 35–40, June 1999.
[19] C. C. Wu, C. I. Wu, J. C. Sturm, and A. Kahn, "Surface modification of indium tin oxide by plasma treatment: an effective method to improve the efficiency, brightness, and reliability of organic light emitting devices," *Appl. Phys. Lett.*, vol. 70, no. 11, pp. 1348–1350, 1997.
[20] M. G. Mason, L. S. Hung, C. W. Tang, S. T. Lee, K. W. Wong, and M. Wang, "Characterization of treated indium–tin–oxide surfaces used in electroluminescent devices," *J. Appl. Phys.*, vol. 86, no. 3, pp. 1688–1692, 1999.
[21] J. S. Kim, R. H. Friend, and F. Cacialli, "Surface energy and polarity of treated indium–tin–oxide anodes for polymer light-emitting diodes studied by contact-angle measurements," *J. Appl. Phys.*, vol. 86, no. 5, pp. 2774–2778, 1999.
[22] J. S. Kim, M. Grnstrom, R. H. Friend, N. Johansson, W. R. Salaneck, R. Daik, W. J. Feast, and F. Cacialli, "Indium–tin oxide treatments for single- and double-layer polymeric light-emitting diodes: The relation between the anode physical, chemical, and morphological properties and the device performance," *J. Appl. Phys.*, vol. 84, no. 12, pp. 6859–6870, 1998.
[23] M. Bernius, M. Inbasekaran, E. Woo, W. Wu, and L. Wujkowski, "Fluorene-based polymers-preparation and applications," *J. Mater. Sci. Mater. Electron.*, vol. 11, pp. 111–116, 2000.
[24] Y. Hong and J. Kanicki, "Integrating sphere CCD-based measurement method of organic light-emitting devices," *Rev. Sci. Instrum.*, vol. 78, no. 7, pp. 3572–3575, 2003.
[25] S. M. Sze, *Physics of Semiconductor Devices*, 2nd ed. New York: Wiley, 1981.
[26] Y. Hong and J. Kanicki, "Organic polymer light-emitting devices on flexible plastic substrates for AM-OPLED," in *Proc. Asia Display*, 2001, pp. 1443–1446.
[27] A. J. Campbell, D. D. C. Bradley, and H. Antoniadis, "Quantifying the efficiency of electrode for positive carrier injection into poly (9,9-dioctylfluorene) and representative copolymers," *J. Appl. Phys.*, vol. 89, no. 6, pp. 3343–3351, 2001.
[28] J. Tauc, *Amorphous and Liquid Semiconductors*, J. Tauc, Ed. New York: Plenum, 1974.
[29] J. Tauc, R. Grigorovici, and A. Vancu, *Phys. Stat. Sol.*, vol. 15, pp. 627–637, 1966.
[30] J. C. Scott, G. G. Malliaras, W. D. Chen, J.-C. Breach, J. R. Salem, S. B. Sachs, and C. E. D. Chidsey, "Hole limited recombination in polymer light-emitting diodes," *Appl. Phys. Lett.*, vol. 74, no. 11, pp. 1510–1512, 1999.
[31] P. W. M. Blom and M. C. J. M. Vissenberg, "Charge transport in poly (p-phenylene vinylene) light-emitting diodes," *Mater. Sci. Eng.*, vol. 27, pp. 53–94, 2000.
[32] W. R. Salaneck and J. L. Bredas, "Conjugated polymer surfaces and interfaces for light-emitting devices," *MRS Bull.*, pp. 46–51, June 1997.
[33] R. H. Friend, R. W. Gymer, A. B. Homes, J. H. Burroughes, R. N. Marks, C. Taliani, D. D. C. Bradley, D. A. Dos Santos, J. L. Bredas, M. Logdlund, and W. R. Salaneck, "Electroluminescence in conjugated polymers," *Nature*, vol. 397, pp. 121–128, 1999.
[34] A. B. Chwang, R. C. Kwong, and J. J. Brown, "Graded mixed-layer organic light-emitting devices," *Appl. Phys. Lett.*, vol. 80, no. 5, pp. 725–727, 2002.
[35] D. Ma, C. S. Lee, S. T. Lee, and L. S. Hung, "Improved efficiency by a graded emissive region in organic light-emitting devices," *Appl. Phys. Lett.*, vol. 80, no. 19, pp. 3641–3643, 2002.
[36] P. K. H. Ho, J. S. Kim, J. H. Burroughes, H. Becker, S. F. Y. Li, T. M. Brown, F. Cacialli, and R. H. Friend, "Molecular-scale interface engineering for polymer light-emitting diodes," *Nature*, vol. 404, pp. 481–484, 2000.
[37] J. Morgado, R. H. Friend, and F. Cacialli, "Improved efficiency of light-emitting diodes based on polyfluorene blends upon insertion of a poly (p-phenylene vinylene0 electron-confinement layer," *Appl. Phys. Lett.*, vol. 80, no. 14, pp. 2436–2438, 2002.
[38] P. W. M. Blom, M. J. J. de Jong, and J. J. M. Vleggaar, "Electron and hole transport in poly (p-phenylene vinylene) devices," *Appl. Phys. Lett.*, vol. 68, no. 23, pp. 3308–3310, 1996.
[39] P. E. Burrows, Z. Shen, V. Bulovic, D. M. McCarty, S. R. Forrest, J. A. Cronin, and M. E. Thompson, "Relationship between electroluminescence and current transport in organic heterojunction light-emitting devices," *J. Appl. Phys.*, vol. 79, no. 10, pp. 7991–8006, 1996.

[40] I. D. Parker, "Carrier tunneling and device characteristics in polymer light-emitting diodes," *J. Appl. Phys.*, vol. 75, no. 3, pp. 1656–1666, 1994.
[41] J. W. T. Walsh, *Photometry*. London, U.K.: Constable, 1958.
[42] I. S. Millard, "High-efficiency polyfluorene polymers suitable for RGB applications," *Synth. Met.*, vol. 111–112, pp. 119–123, 2000.
[43] M. Leadbeater, "Polymers shine the light," *Oemagazine*, vol. 2, no. 6, pp. 14–17, 2002.
[44] M. T. Bernius, M. Inbasekaran, J. O'Brien, and W. Wu, "Progress with light-emitting polymers," *Adv. Mater.*, vol. 12, no. 23, pp. 1737–1750, 2000.
[45] K. Xing, M. Fahlman, M. Logdlund, D. A. dos Santos, V. Parente, R. Lazzaroni, J. L. Bredas, R. W. Gymer, and W. R. Salaneck, "The interaction of poly (p-phenylenevinylene) with air," *Adv. Mater.*, vol. 8, no. 12, pp. 971–974, 1996.

Yongtaek Hong (S'95–M'04) was born in Busan, Korea, in 1971. He received B.S. and M.S. degrees in electronics engineering from Seoul National University, Seoul, Korea, in 1994 and 1996, respectively and the Ph.D. degree in electrical engineering from the University of Michigan, Ann Arbor, in 2003.

He is currently with the Display Science and Technology Center, Eastman Kodak Company, Rochester, NY, as a Senior Research Scientist. His research interests are low-cost back plane technologies for robust, flexible flat panel displays and digital radiography sensor arrays. Based on his Ph.D research regarding a-Si:H TFT active-matrix polymer light-emitting displays, he authored and coauthored more than 20 journal papers and conference presentations.

Dr. Hong received the Korea Foundation for Advanced Studies Scholarship from 1997 to 2002, and the College of Engineering Graduate Student Distinguished Achievement Awards from the University of Michigan in 2003. He is a member of SID and SPIE.

Jerzy Kanicki (M'99–A'99–SM'00) received the Ph.D. degree in sciences (D.Sc.) from the Universit Libre de Bruxelles, Brussels, Belgium, in 1982.

He subsequently joined the IBM Thomas J. Watson Research Center, Yorktown Heights, NY, as a Research Staff Member working on hydrogenated amorphous silicon devices for the photovoltaic and flat-panel display applications. In 1994, he moved from the IBM Research Division to the University of Michigan, Ann Arbor, as a Professor in the Department of Electrical Engineering and Computer Science (EECS). His research interests within the Electrical and Computer Engineering (ECE) Division of the EECS include organic and molecular electronics, TFTs and circuits, and flat-panel displays technology, including organic light-emitting devices.